# Analysis of Delayed Failure in Sloping Excavations

By D. V. Griffiths,[1] Member, ASCE, and C. O. Li[2]

**Abstract:** The paper describes a finite element technique that takes account of transient effects through a Biot analysis, enabling coupling of pore pressure variations to a nonlinear soil stress-strain law. The algorithm can retrieve both drained and undrained solutions as special cases and has been verified against some existing solutions for time-dependent failure of soil masses. The technique is then applied to the transient stability of excavated soil slopes. Long-term instability is modeled by allowing the pore suctions, initially generated by the excavation process, to dissipate. For the slope under analysis, the coefficient $K_0$ is seen to have a significant influence on the undrained (short-term) factor of safety, but little effect on the drained (long-term) value.



## INTRODUCTION

The stability of foundations and earthworks in saturated fine-grained soils is a time-dependent process. This is because any change in total normal stress is initially resisted by pore pressures, which then dissipates over a period of time. The rate of this dissipation is greatly influenced by the permeability of the soil and the length of the drainage paths in the soil mass. A fine-grained soil such as clay may take a very long time for the pore pressures to dissipate, whereas in a coarse-grained soil such as gravel the pore pressures reach equilibrium almost immediately. Between these extremes lie silts and fine sands, where the permeability is sufficiently low to require a finite amount of time for pore pressure dissipation. Fine-grained cohesionless soils are particularly susceptible to stability problems caused by temporary generation of compressive pore pressures.

In the case of saturated soils with a compressible skeleton (i.e., normally consolidated clay), increases in shear stress tend to cause the soil skeleton to contract, which in turn are resisted by compressive pore pressures in the voids of the soil. As the pore water flows out of these highly stressed areas, the pressures dissipate, and the effective stresses rise leading to an increase in shear strength. This type of situation is a "short-term" stability problem, because the minimum factor of safety against failure occurs immediately after the loads are applied.

"Long-term" stability problems occur when an initial reduction in pore pressure is induced in the soil. This might be caused by unloading, such as that which occurs after excavation, or dilative behavior of dense or overconsolidated soils. In such cases, pore pressures would rise as equilibrium is reached with an accompanying reduction in shear strength and factor of safety. Both these extremes of behavior were originally described by Bishop and Bjerrum (1960).

[1]Sr. Lect., Dept. of Engrg., Univ. of Manchester, Manchester M13 9PL, United Kingdom.

[2]Grad. Student, Dept. of Engrg., Univ. of Manchester, Manchester M13 9PL, United Kingdom.

Note. Discussion open until February 1, 1994. To extend the closing date one month, a written request must be filed with the ASCE Manager of Journals. The manuscript for this paper was submitted for review and possible publication on April 24, 1991. This paper is part of the ***Journal of Geotechnical Engineering***, Vol. 119, No. 9, September, 1993. ©ASCE, ISSN 0733-9410/93/0009-1360/$1.00 + $.15 per page. Paper No. 1828.

In order to avoid the complexities of transient analyses, the problem is customary dealt with by using one of two simplifying assumptions. The first, referred to as an undrained or short-term analysis, aims to define the stress states and displacement fields immediately after loads are applied and before there has been any appreciable drainage. One way of dealing with this in the context of finite element analysis, is to treat the pore fluid as a virtually incompressible material mixed with a compressible soil skeleton. This type of analysis has been implemented using finite element analyses [see, e.g., Naylor (1974) and Griffiths (1985)] for the undrained problem, with a range of constitutive laws governing the soil behavior. The second, referred to as drained or long-term analysis, assumes that the pore pressures have already reached their final steady-state values. As all transient effects have died away, this type of problem is dealt with using more conventional drained analyses, in which the soil is treated as a one-phase material.

In the construction of large earthworks the loading sequence itself will usually be time-dependent. Typically, the loading would be gradually increased (i.e., staged construction) until a maximum value is reached that then remains constant. On such occasions, it may be desirable to analyze the coupled performance of the soil in which the two phases interact.

An application for which it is important to consider the implications of transient loading occurs in the dredging of soils where the *rate* of excavation can affect the amount of power required to remove a given quantity of soil (van Leussen and Niewenhuis 1984). A simple example of this type is given later in the paper in order to verify the coupled algorithm. Other applications include the estimation of the holding capacity of anchors for ships and offshore structure. In such systems, the passive resistance of the saturated soils is of direct relevance to the anchor capacity.

## DELAYED FAILURE OF SLOPES

The delayed failure of slopes has been a subject of considerable interest to soil mechanics research workers and practitioners for a number of years [see, e.g., Henkel (1957), Skempton (1977), and Bromhead (1986)]. In Britain, study of the problem has focused on London clay, which can be classified as stiff and overconsolidated. Delayed failure of slopes cut in such materials must occur due to a gradual reduction of shear strength, for which various explanations have been offered. Terzaghi (1936) suggested that the decrease in soil strength with time might be due to softening of the material, caused when an applied shear stress is associated with a reduction in lateral stress as in the case of a cutting. Henkel (1957) thought that local shear failure in the vicinity of open fissures might play a major part in explaining the reduction in strength with time.

Further contributions to the understanding of delayed failure in overconsolidated clays were made by Vaughan and Walbancke (1973) and Skempton (1977). From the analyses of various case histories carried out in terms of effective stress with pore pressure measurement, it was recognized that the very slow equilibration of pore suctions following excavation played an important part in the explanation of delayed failure. It is this suggested mechanism that motivated the program development and subsequent analyses presented in this paper.

## TRANSIENT ANALYSIS INCORPORATING PLASTICITY

This paper uses the Biot (1941) formulation to study the coupled interactions between the solid and fluid phases. This approach, which treats the

soil as a two-phase material, has been used successfully in several geotechnical applications, usually involving linear soil models [see, e.g., Hwang et al. (1971) and Smith and Hobbs (1976)]. Nonlinear soil models have also been incorporated into the Biot formulation, for example by Small et al. (1976) in analyzing boundary value problems using an elastic-perfectly plastic Mohr-Coulomb constitutive law and by Hicks and Smith (1986) in which a double-hardening model was considered.

Numerical and analytical results relating to a transient passive earth-pressure problem (Li 1988; Griffiths and Li 1989) are used to verify the method proposed in this paper. The method is subsequently applied to stability problems of excavated soil slopes. A detailed description of the algorithm can be found elsewhere [e.g., Li (1988) and Smith and Griffiths (1988)], but a brief description of the governing equations is presented in the next section.

The nonlinear soil behavior is assumed to be elastic-perfectly plastic with a Mohr-Coulomb failure criterion and is modeled using a "viscoplastic" algorithm [see, e.g., Zienkiewicz et al. (1975)]. Each time step of the transient behavior is treated as a pseudo-static analysis within which stresses that have violated the failure criterion are redistributed in an iterative manner.

The Biot and Viscoplastic formulations are described in some detail in other publications, and the coding for both, together with details of the finite difference time-stepping algorithms is published in full in the text by Smith and Griffiths (1988).

The fully coupled Biot formulation can be expressed in a variety of ways depending on the time-stepping algorithm to be used. In the present work, a fully "implicit" approach is used together with an incremental formulation suggested by Hicks (1990). The governing differential equations in two dimensions are given by:

Equilibrium:

$$\frac{\partial \sigma_x'}{\partial x} + \frac{\partial \tau_{xy}}{\partial y} + \frac{\partial u_w}{\partial x} = 0 \quad \ldots\ldots (1)$$

$$\frac{\partial \tau_{xy}}{\partial x} + \frac{\partial \sigma_y'}{\partial y} + \frac{\partial u_w}{\partial y} = 0 \quad \ldots\ldots (2)$$

Continuity and Darcy's Law:

$$\frac{k_x}{\gamma_w}\frac{\partial^2 u_w}{\partial x^2} + \frac{k_y}{\gamma_w}\frac{\partial^2 u_w}{\partial y^2} + \frac{\partial}{\partial t}\left(\frac{\partial u}{\partial x} + \frac{\partial v}{\partial y}\right) = 0 \quad \ldots\ldots (3)$$

which lead to the following matrix version of the Biot equations at the element level:

$$\begin{bmatrix} \mathbf{k}_m & \mathbf{c} \\ \mathbf{c}^T & -\Delta t \theta \mathbf{k}_p \end{bmatrix} \begin{Bmatrix} \Delta \mathbf{r} \\ \Delta \mathbf{u}_w \end{Bmatrix} = \begin{Bmatrix} \Delta \mathbf{f} \\ \Delta t \mathbf{k}_p u_{w_0} \end{Bmatrix} \quad \ldots\ldots (4)$$

where $\sigma_x'$, $\sigma_y'$, $\tau_{xy}$ = effective stresses; $u_w$ = excess pore pressure; $u$, $v$ = deformations in $x$- and $y$-directions; $k_x$, $k_y$ = coefficients of permeability in $x$- and $y$-directions; $\gamma_w$ = unit weight of water; $\mathbf{k}_m$ = element solid stiffness matrix; $\mathbf{k}_p$ = element fluid "stiffness" matrix; $\mathbf{c}$ = element coupling matrix; $\Delta \mathbf{r}$ = change in nodal displacements; $\Delta \mathbf{u}_w$ = change in nodal excess pore

pressures; $\mathbf{u}_{w_0}$ = "old" excess pore pressures; $\Delta\mathbf{f}$ = change in nodal forces; $\Delta t$ = calculation time step; and $\theta$ = time stepping parameter (= 1 in present work).

After assembly into the global system, this time-stepping algorithm is unconditionally stable, but requires repeated solution of simultaneous equations. An advantage of this approach rather than "explicit" ($\theta = 0$) methods is that the long-term or steady-state solution can be achieved in a single large time step provided the left-hand-side matrix in (4) remains constant.

In all the analyses presented in this paper, the finite element meshes consisted of eight-noded elements for the solid (soil) phase and four-noded elements for the fluid phase (Zienkiewicz 1977). Two-point Gaussian quadrature has been used throughout.

## ALGORITHM VERIFICATION-PASSIVE EARTH PRESSURE

To test the algorithm, it is first applied to a problem for which solutions have already been obtained. The analysis chosen is that of a plane strain passive earth pressure problem in which a smooth wall is translated horizontally into a bed of saturated soil at varying speeds. This type of analysis may also represent, for example, a simple model of dredging in which a cutting blade removes saturated soil from an underwater location. The finite element mesh is shown in Fig. 1. All boundaries of the mesh are impermeable except the top surface at which drainage can occur. The soil is saturated with shear strength defined by Mohr-Coulomb with parameters $c'$ and $\phi'$. The problem is to estimate the ultimate passive resistance offered by the soil as a function of the rate at which the wall is translated into the soil.

The soil is given the following properties in which primes denote quantities defined with respect to effective stresses: $E' = 1 \times 10^4$ kPa; $\nu' = 0.25$; $c' = 0$ kPa; $\phi' = 30°$, ($K_p = 3$); $\gamma' = 10$ kN/m$^3$; $K_0 = 0.5$; $k/\gamma_w = 0.86$ m$^4$/(kN day) (isotropic); and $c_v = 1.04 \times 10^4$ m$^2$/day.

The Biot formulation leads to the soil permeability $k$ and the unit weight of water $\gamma_w$ being combined in the ratio $k/\gamma_w$. For the remainder of the paper this ratio will be retained; however, as $\gamma_w \approx 10$ kN/m$^3$ the ratio is approximately 10 times smaller than the actual permeability of the soil.

Computation of failure loads is the priority in the present work, so no

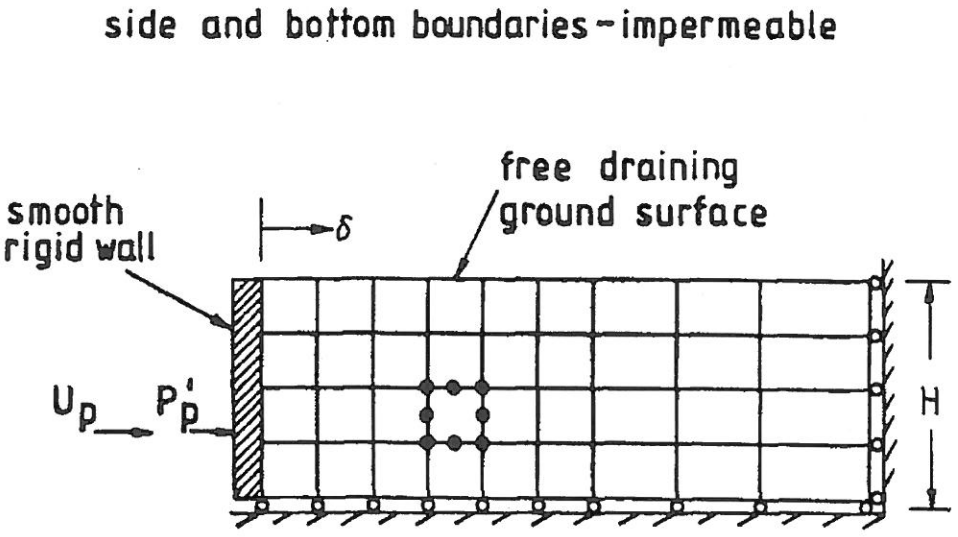


**FIG. 1. Mesh Used for Earth Pressure Analyses**

real attempt has been made to model accurately soil deformations. Although the value of Young's modulus attributed to the soil is arbitrary, it will be approximately proportional to the computed deformations. Hence, if more realistic soil moduli were available the resulting deformations could be approximated by simple scaling.

The soil mass is assumed to be fully saturated, with initial effect stresses given by the product of the submerged unit weight and the depth of each Gauss point below the soil surface.

A dimensionless parameter $L_R$ is used to represent the (constant) speed of the wall as it translates into the soil. This quantity is given by (see Fig. 1):

$$L_R = \frac{d\left(\frac{\delta}{H}\right)}{dT_d} \quad \ldots\ldots (5)$$

where a dimensionless time factor is defined in the usual way in terms of the coefficient of consolidation, time, and a reference length (in this case the height of the wall)

$$T_d = \frac{c_v t}{H^2} \quad \ldots\ldots (6)$$

and the coefficient of consolidation is a function of the effective elastic properties, the coefficient of permeability, and the unit weight of water

$$c_v = \frac{k(1 - \nu')E'}{\gamma_w(1 - 2\nu')(1 + \nu')} \quad \ldots\ldots (7)$$

The permeability is assumed to be isotropic, hence $c_v = c_h$. The height of the wall is $H$ and $\delta$ represents the distance moved by the wall after time $t$.

Assuming a nondilative soil ($\psi' = 0°$), the computed effective passive force exerted by the soil on the wall for three different wall speeds is shown in Fig. 2. These plots show the buildup of effective force $P'_p$ as the wall is displaced into the soil. The "fast," "intermediate," and "slow" cases correspond to $L_R = 1.0$, 0.01, and 0.0001, respectively.

In the undrained case (fast loading), the maximum passive force has been given by Griffiths and Li (1988) as:

$$P'_p = \frac{1}{2}\gamma' H^2 \frac{K_p(K_0 + 1)}{K_p + 1} \quad \ldots\ldots (8)$$

and in the drained case (slow loading) by the simple Rankine solution:

$$P'_p = \frac{1}{2}\gamma' H^2 K_p \quad \ldots\ldots (9)$$

The finite element results were in close agreement with both these solutions. As expected, the intermediate loading case ($L_R = 0.01$) gave a value of $P'_p$, which would eventually level out between the drained and undrained limits. The form of this curve differs from the other two due to the simultaneous buildup and dissipation of pore pressures as the wall is displaced. Further results relating to this problem, including the effects of dilatancy, were reported by Griffiths et al. (1992).

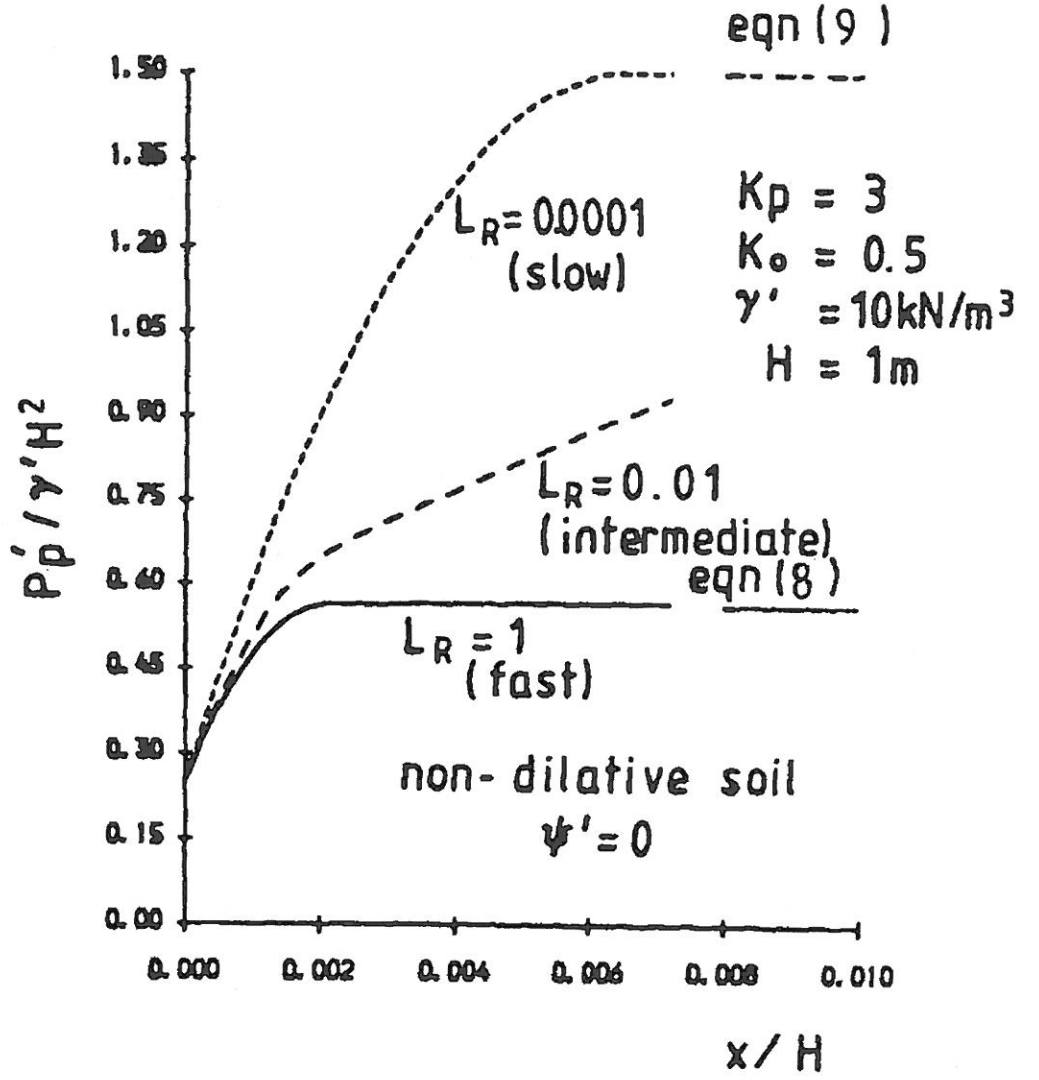


**FIG. 2. Effective Force versus Displacement, for Different Wall Speeds**

## ANALYSIS OF UNDERWATER EXCAVATION

The transient stability of the 2:1 slope shown in Fig. 3 is now analyzed using the same program as was employed for the earth pressure case described previously. Excavation is assumed to take place by the sudden removal of material above the surface ABC. Excavation is carried out under water, and the soil mass is saturated with initial stresses due to its effective self-weight. The ground water is assumed to remain at the crest level throughout. The excavation loads applied to surface ABC in Fig. 3 are assumed to take one day to fully develop. The loads are computed by determining the initial stresses acting on the excavation surface prior to excavation, and computing a consistent set of equal and opposite nodal forces.

The transient stability of the slope is then studied as the excess pore pressures generated by the excavation process dissipate. The properties assumed in the slope shown in Fig. 3 are as follows: $E' = 2 \times 10^5$ kPa; $v' = 0.25$; $c' = 3$ kPa; $\phi' = 20°$; $\psi' = 0°$; $\gamma' = 10$ kN/m$^3$; $\gamma_w = 10$ kN/m$^3$; $K_0 = 0.5$ and 1.5; $k/\gamma_w = 8.64 \times 10^{-5}$ m$^4$/(kN day) (isotropic); and $c_v = 20.7$ m$^3$/day.

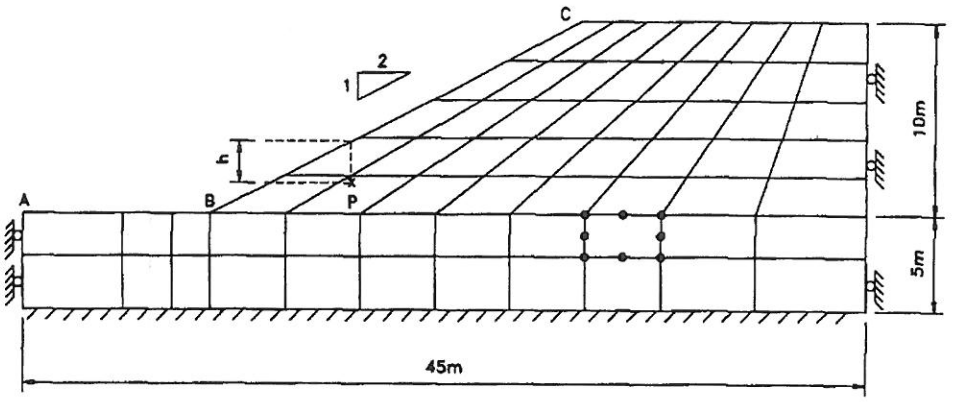


**FIG. 3. Mesh Used for Excavation Analyses**

At any subsequent time after excavation, the factor of safety (FOS) of the slope is defined as the factor applied to the peak shear strength of the soil in order to cause a general shear failure. It is assumed here that the same factor is applied to both $c'$ and $\tan \phi'$, thus the factored strength parameters actually being used in the analysis are given by: $\phi_f' = \arctan(\tan \phi'/\text{FOS})$ and $c_f' = c'/\text{FOS}$.

On this basis, the drained factor of safety of the slope considered here as given by Bishop and Morgenstern (1960) is 1.16. In order to compare with this drained result, a factor of safety of 1.2 was used to obtain the factor shear strength parameters $\phi_f'$ and $c_f'$, which were then used in the finite element analysis. This could be expected to cause failure in the long term, but in the short term the slope would have a higher factor of safety and remain stable.

Deformations of the excavated slope corresponding to different time intervals for the cases, when $K_0 = 0.5$ and $K_0 = 1.5$ are given in Figs. 4 and 5, respectively. These two cases are intended to be generally representative of a normally consolidated and a lightly overconsolidated soil, respectively. In the case of a low $K_0 = 0.5$ (Fig. 4), the slope failed after six days with a failure mechanism characterized by significant crest and toe displacements. In the case of a higher $K_0 = 1.5$ (Fig. 5), the slope failed after 15 days by excess heave at the bottom of the excavation with little crest movement. The deformations shown in Figs. 4 and 5 correspond to the elasto-plastic deformations of the slopes at different times following excavation. Although the constitutive model allowed no plastic volume change ($\psi' = 0$), the effective Poisson's ratio of 0.25 would allow volume increase to occur in the long-term following unloading. These volume changes have been exaggerated by a scaling factor for the sake of clarity.

To explain this difference, the fully drained and undrained factors of safety for the slope were computed for both values of $K_0$. In each case, the factor of safety was gradually increased (with a corresponding reduction in factored shear strength values) until "failure" occurred as indicated by a sudden increase in nodal displacements.

These results, in the form of toe displacement versus FOS, are given in Figs. 6(*a*)–6(*d*). Figs. 6(*a*) and 6(*c*) confirm that the high initial effective stresses when $K_0 = 1.5$, result in a greater undrained strength than when $K_0 = 0.5$, the factors of safety being calculated at approximately 3 and 1.6, respectively. The results in Figs. 6(*b*) and 6(*d*), however, show that the initial stresses have little effect on the drained stability of the slope, with both cases predicting a factor of safety close to the Bishop and Morgenstern

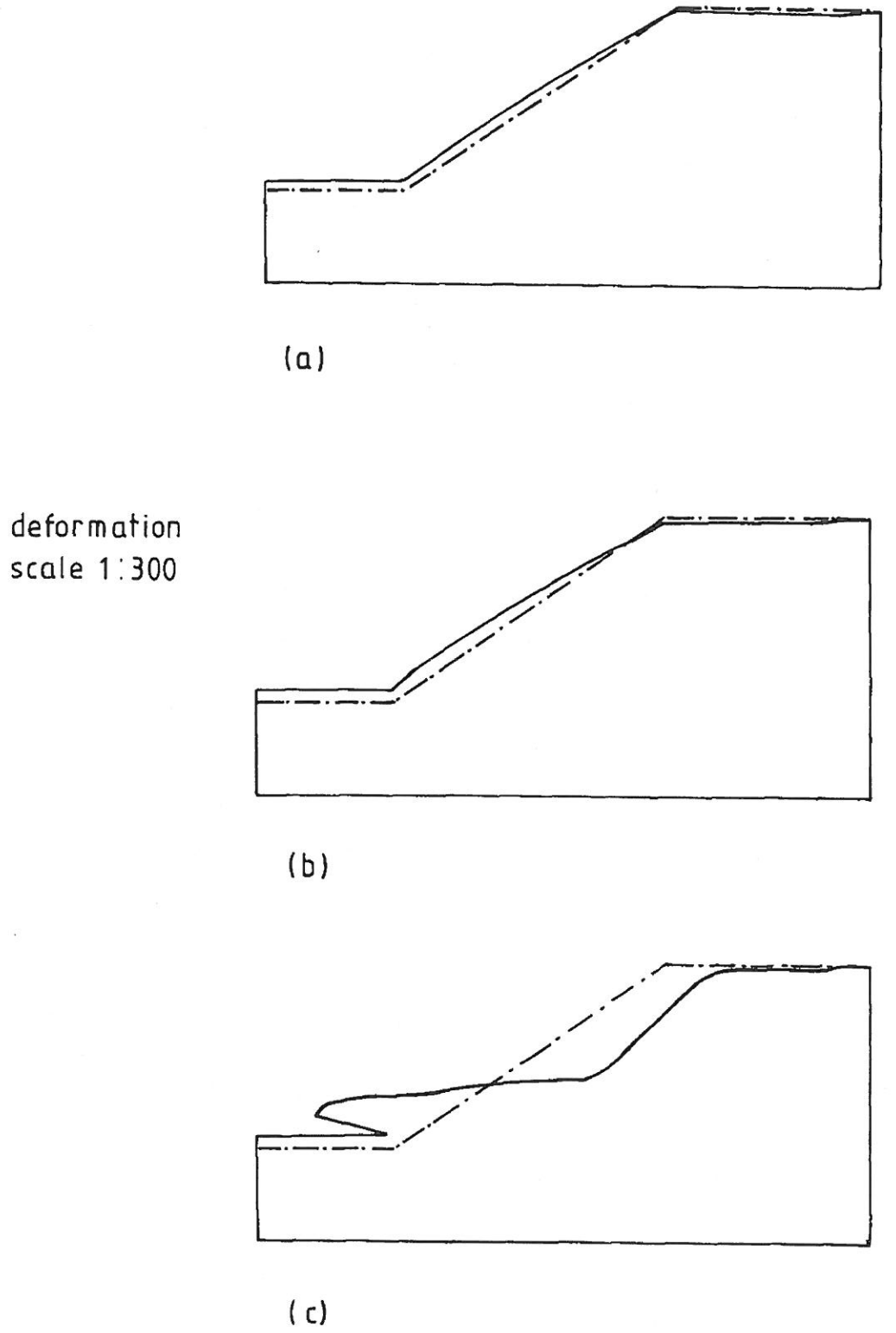


**FIG. 4. Surface Deformations Following Excavation ($K_o$ = 0.5): (*a*) Immediately after Excavation; (*b*) One Day after Excavation; and (c) Six Days after Excavation**

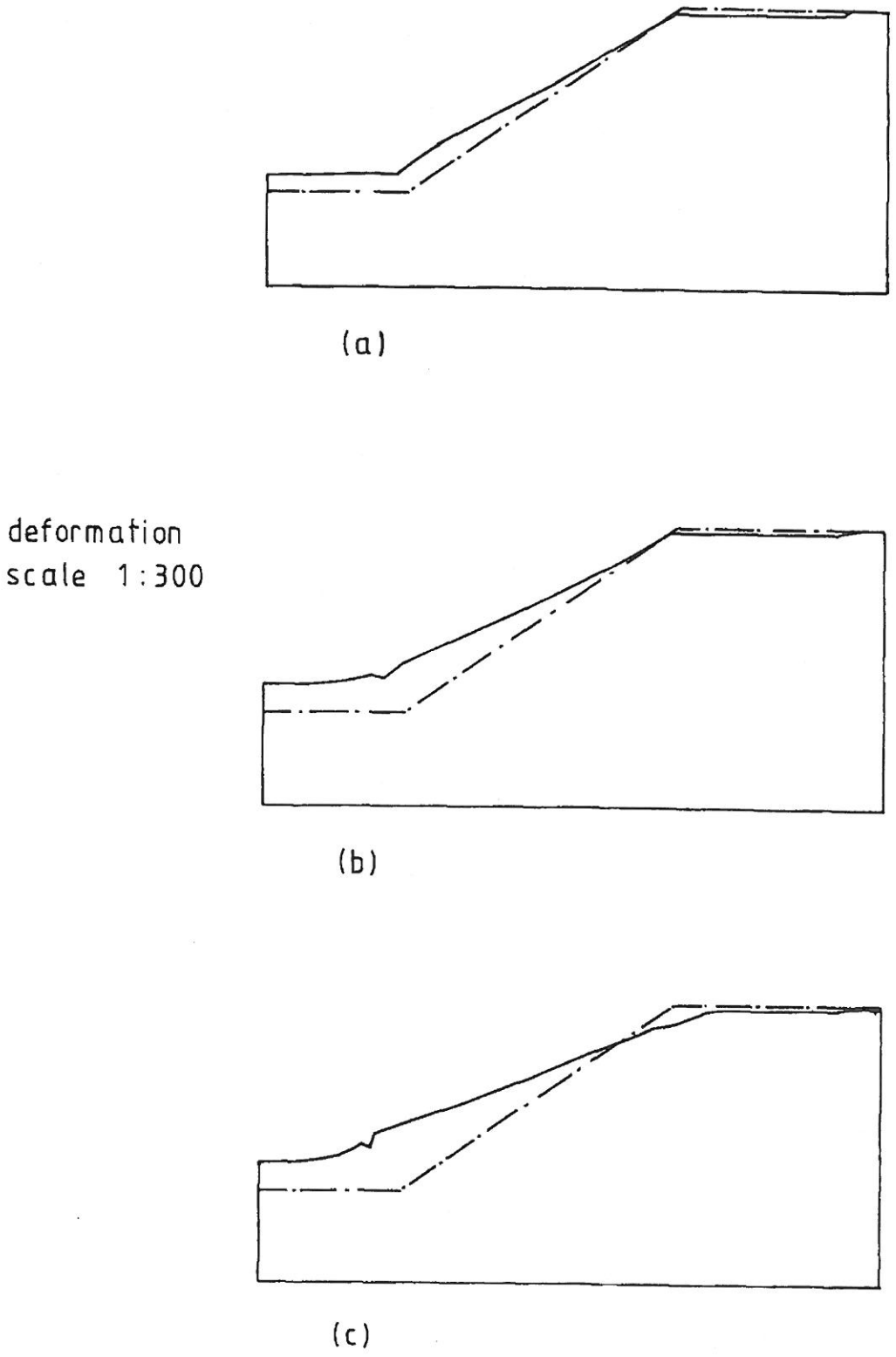


**FIG. 5. Surface Deformations Following Excavation ($K_0$ = 1.5): (*a*) Immediately after Excavation; (*b*) Four Days after Excavation; and (*c*) 15 Days after Excavation**

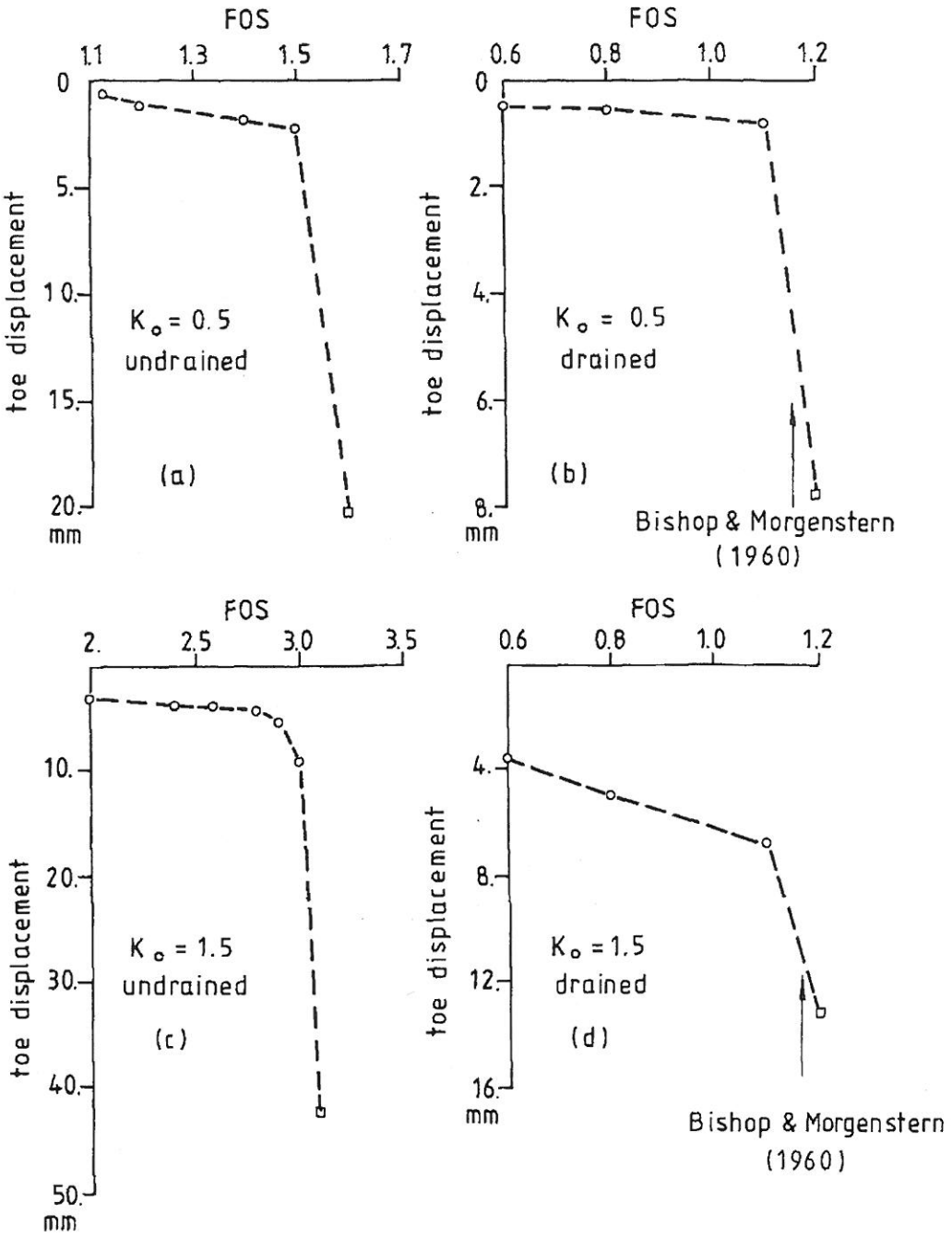


**FIG. 6. Undrained and Drained Factors of Safety**

value. It is noted that in both the drained and undrained cases, relatively larger toe displacements at failure are observed in the soil with the higher value of $K_0$. It should be pointed out though, that the same Young's modulus was used for both the analyses, so the additional soils stiffness that would be expected with the higher value of $K_0$ has not been modeled here.

In order to further investigate the transient stability of the slope for a fixed factor of safety, horizontal toe displacements were observed as a function of time for FOS equal to 1.1 and 1.2, respectively. These values were chose because they lie on either side of the "correct" factor of safety for the drained case of 1.16.

Fig. 7 shows the horizontal toe displacements as a function of time when

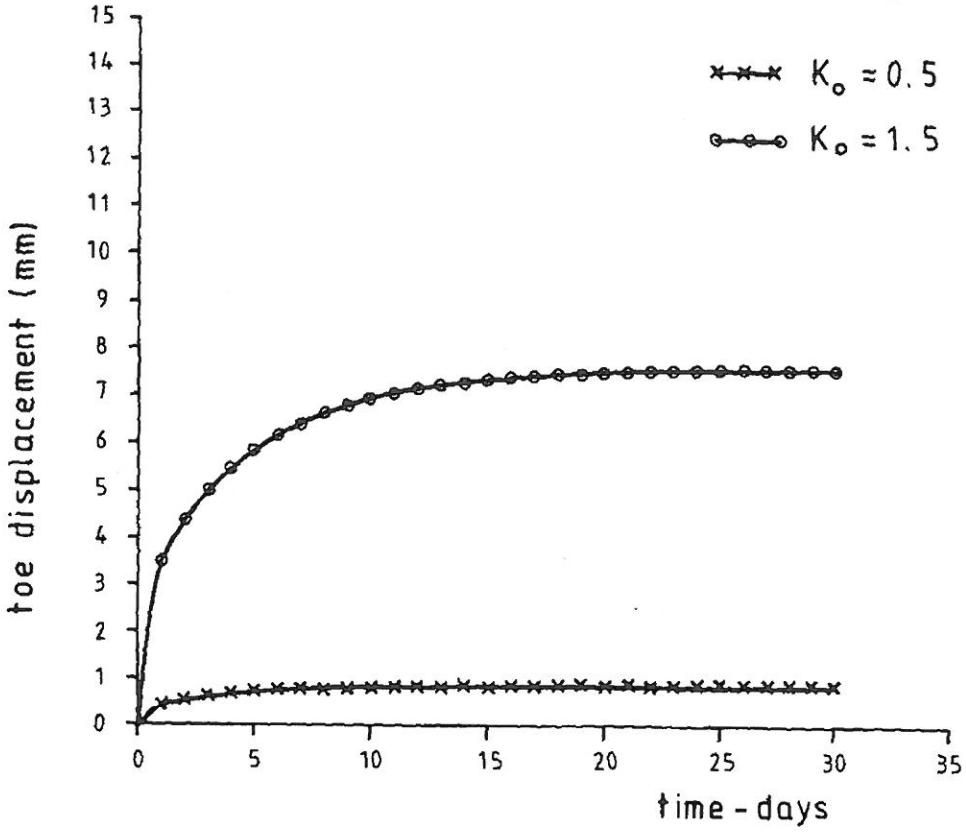


**FIG. 7. Time versus Toe Displacement, (FOS = 1.1)**

the soil properties are factored by 1.1. In this case, as the factored soil properties are still sufficient to support the weight of the slope in the long term, the displacements level out at their equilibrium values after a few days. Fig. 8 shows the horizontal toe displacements as a function of time when the soil properties are factored by 1.2. In this case, a dramatic increase in displacements occurs after six and 15 days in the "normally consolidated" and "overconsolidated" cases, respectively.

An alternative way of presenting these results is shown in Fig. 9, where the factor of safety of the slope is plotted as a function of time. In the long term, both cases exhibit a factor of safety close to 1.2, but in the short term, the "overconsolidated" clay gave a higher factor of safety than the normally consolidated clay as already implied by Figs. 6(*a*) and 6(*c*).

Fig. 10 shows the variation of normalized effective overburden pressure and excess pore pressure with time at point *P* within the slope (see Fig. 3). The removal of overburden pressure by excavation results in an immediate reduction in pore pressure. The soils that make up the slope experience a temporary increase in shear strength due to the consequent rise in mean effective confining pressure. In the long term, the pore pressures return to the equilibrium value governed by the prevailing ground-water table, in this case assumed to be unchanged at the crest level of the slope. As the pore pressures rise to their equilibrium values, the soil shear strength falls, thus the factor of safety is at a minimum in the long term.

## EFFECT OF $K_0$

Heavily overconsolidated clays, usually have fissures and joints that make them discontinuous. Bjerrum (1967) pointed out that the stress-strain re-

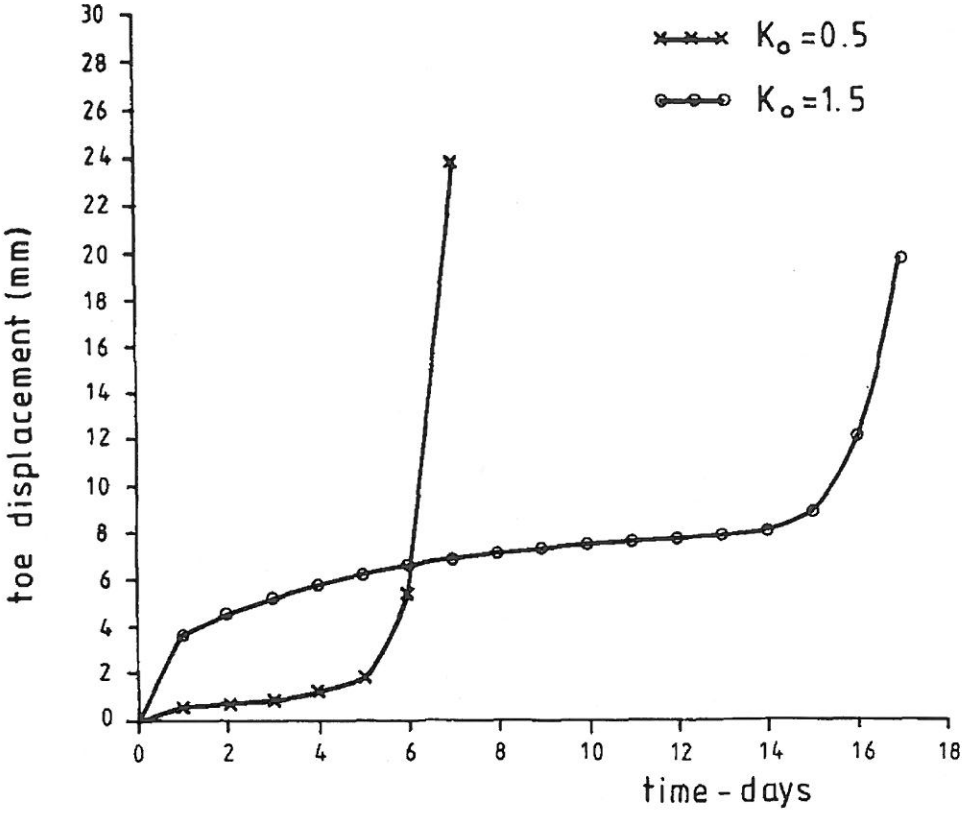


**FIG. 8. Time versus Toe Displacement, (FOS = 1.2)**

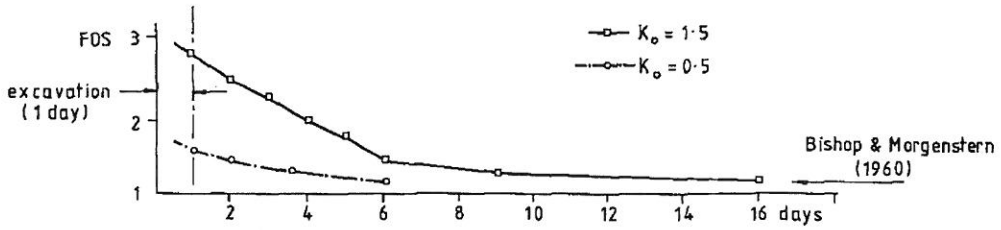


**FIG. 9. FOS versus Time for $K_o$ = 0.5 and $K_o$ = 1.5**

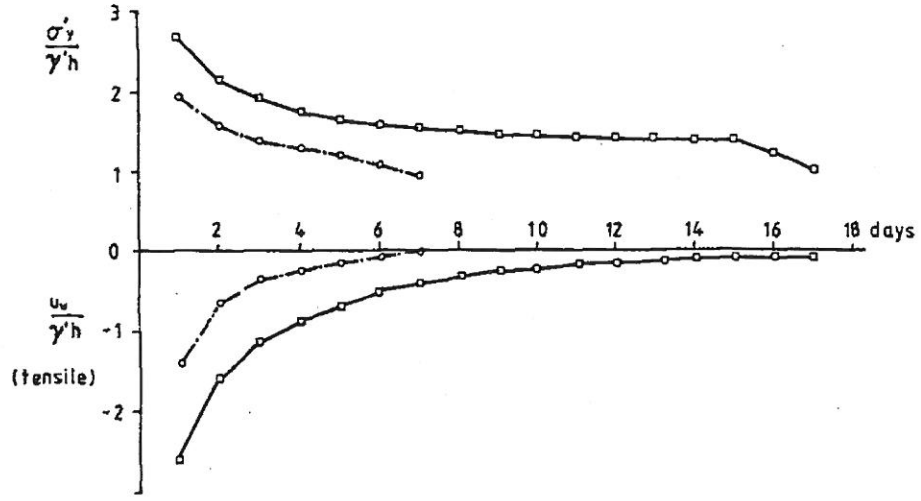


**FIG. 10. Vertical Effective Stress and Pore Pressure versus Time, at Point $P$**

lationship of such soils often displays marked strain softening that complicates the mobilization of shear strength at failure. Skempton (1970) also suggested that the peak shear strength cannot be relied upon in the long term and that the strength of the material decays with time through the reduction of the drained "cohesion" $c'$. As a result, complete understanding of this problem would require a time-dependent solution incorporating a strain-softening material capable of accounting for progressive failure. The simple Mohr-Coulomb model can be adapted to include softening (Griffiths 1981), but in this paper only the "dissipative" contribution to weakening of the soil mass has been considered. In this study, $K_0$ has been varied to assess the influence of initial stress conditions on the behavior of otherwise similar soils.

The higher initial effective stress present when $K_0 = 1.5$ results in higher excavation forces because more stress is "removed," has a higher undrained strength, and hence a higher factor of safety immediately after excavation. Also as shown in Figs. 4 and 5, the long-term mechanism of failure predicted by the analyses differ significantly, with relatively more base movement

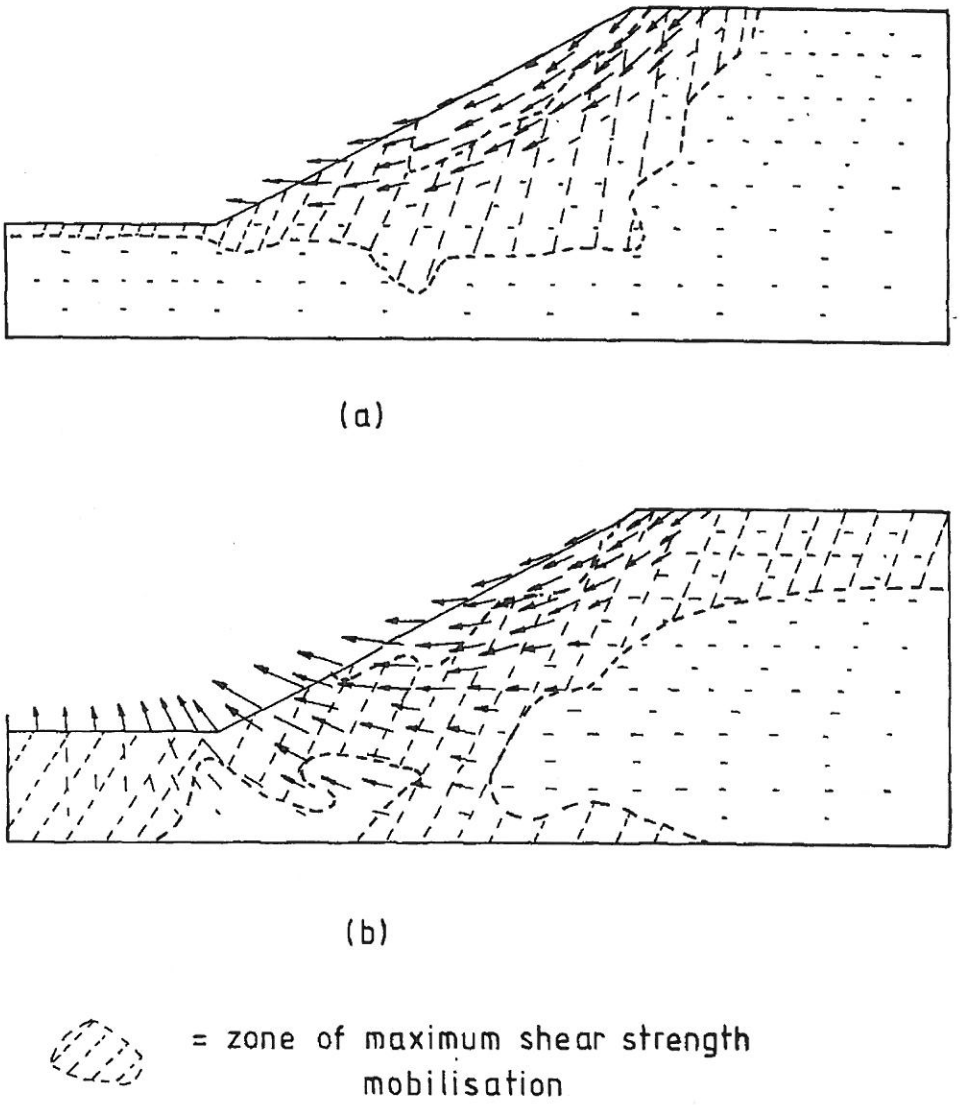


**FIG. 11. Displacement Vectors and Zones of Soil at Failure: (*a*) $K_0 = 0.5$; and (*b*) $K_0 = 1.5$**

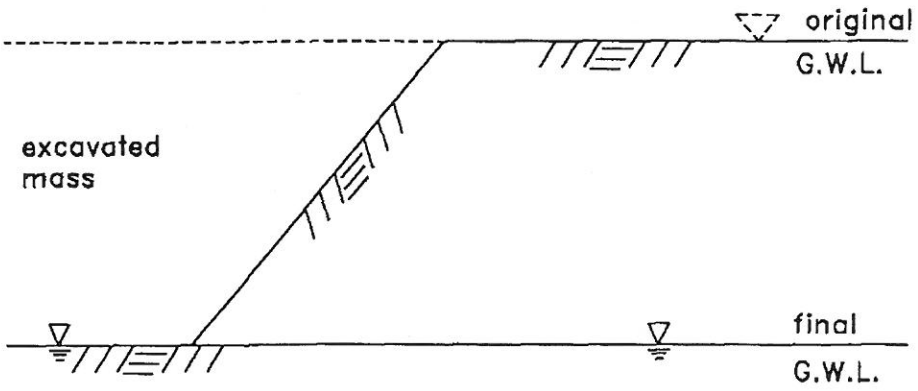


FIG. 12. Simultaneous Excavation and Dewatering

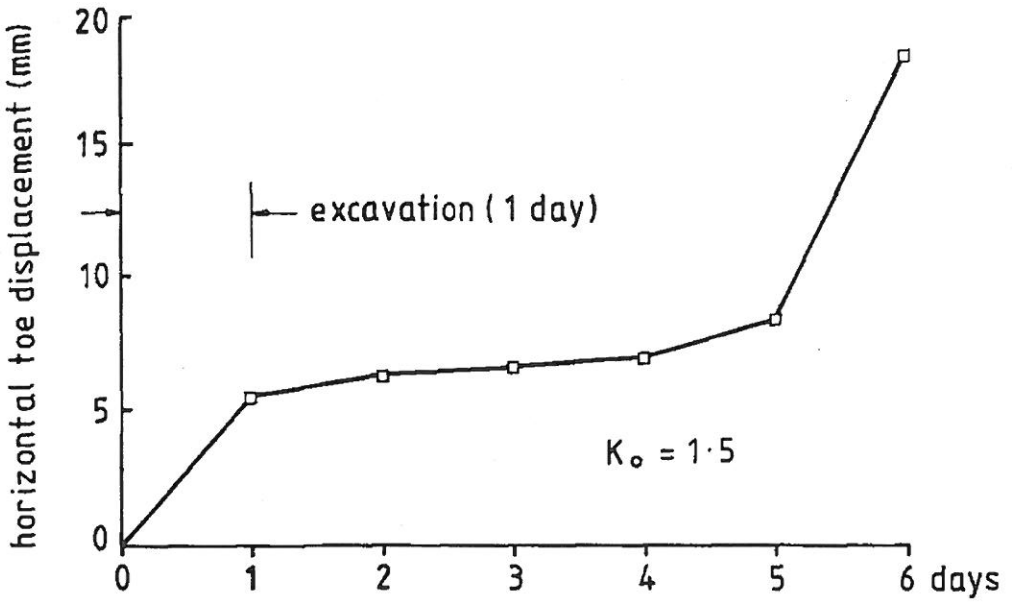


FIG. 13. Time versus Toe Displacement, Following Excavation and Dewatering

observed in the case when $K_0 = 1.5$. Figs. 11(*a*) and 11(*b*) compare the deformation mechanisms and the zones of soil at failure when the slope is on the point of collapse corresponding to a factor of safety of 1.2. The hatched area gives those Gauss points within the FE mesh where failure has occurred according to the Mohr-Coulomb failure criterion. For the lower $K_0$ value [Fig. 11(*a*)], a quite localized (shallow) mechanism occurs, with the zone of yielding soil concentrated in the upper parts of the mesh. For the higher $K_0$ value [Fig. 11(*b*)], a more extensive zone of yielding soil is observed, with consequently greater deformations.

In the overconsolidated case, the initial stress conditions are "closer" to failure than in the normally consolidated soil, hence after unloading, a more extensive zone of soil can be expected to reach failure. Similar observation regarding the influence of $K_0$ have been made with respect to flexible retaining walls by Potts and Fourie (1984).

## EFFECT OF GROUND-WATER LEVEL ON STABILITY

The previous example involved excavation performed underwater, with the long-term ground water maintained at the crest level of the slope. We

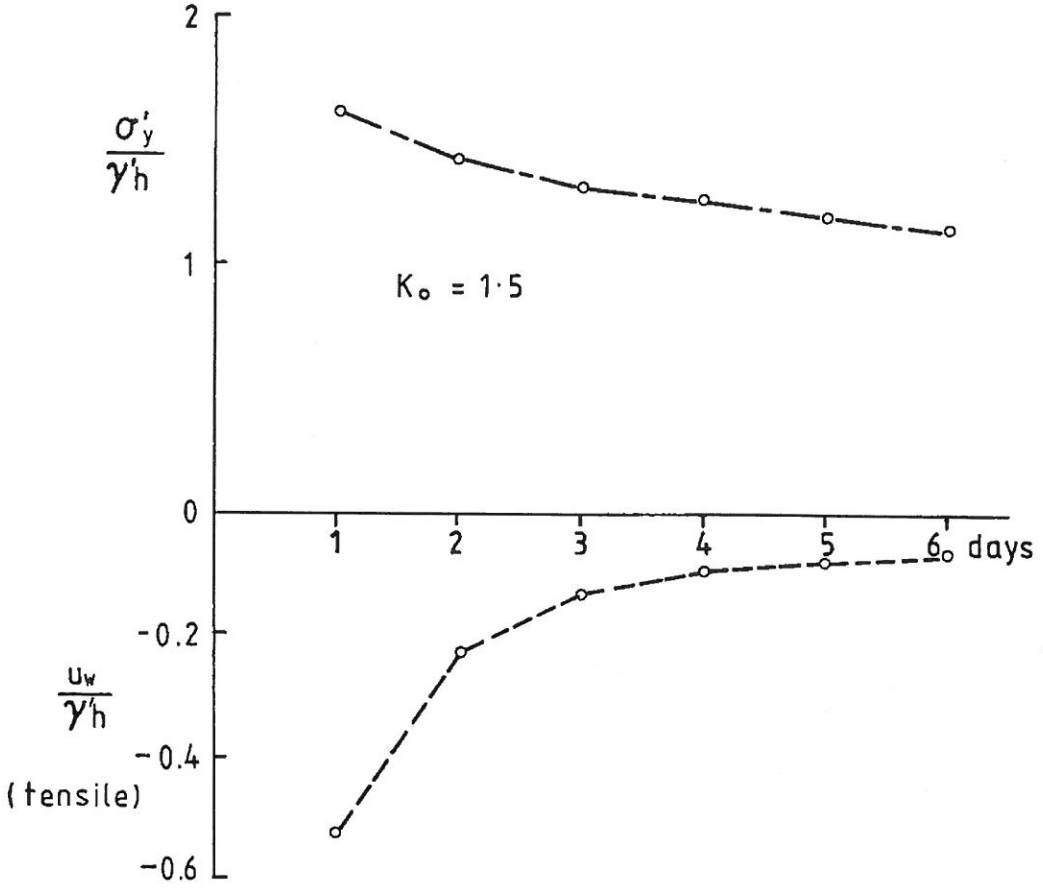


**FIG. 14. Vertical Effective Stress and Pore Pressure versus Time, at Point *P* Following Excavation and Dewatering**

now consider the effects of simultaneous excavation and dewatering as indicated in Fig. 12. As before, a consistent set of nodal loads is applied to the excavated surface equivalent to the removal of the submerged material. In addition, a set of gravity nodal loads are applied to the remaining soil *above* the water table to model the additional weight of this zone of the mesh due its loss of buoyancy. In this case, pore pressure changes are generated by both excavation and dewatering, and subsequent dissipation is based on new boundary conditions where the long-term ground-water level is at the base of the excavation. This process is similar to "rapid drawdown" phenomena where the water level outside the slope is lowered [see, e.g., Li and Griffiths (1988)].

An analysis of this type has been performed on the same mesh as considered previously. In this case only the $K_0 = 1.5$ case was considered, and the factor safety was maintained at unity (FOS = 1.0). The deformation of the toe of the slope as a function of time is shown in Fig. 13. Failure of the slope, as indicated by a sudden increase in the rate of displacement, occurs after five days (four days after completion of excavation). The corresponding variation in vertical effective stress and excess pore pressure at point *P* (Fig. 3), now just above the long-term ground-water level, is shown in Fig. 14. This shows that equilibrium of excess pore pressure gives rise to decreasing effective stress, and hence failure is delayed. The pore pressure dissipation is almost complete after five to six days as compared with 15–16 days in the case when the ground-water level remained unchanged. The

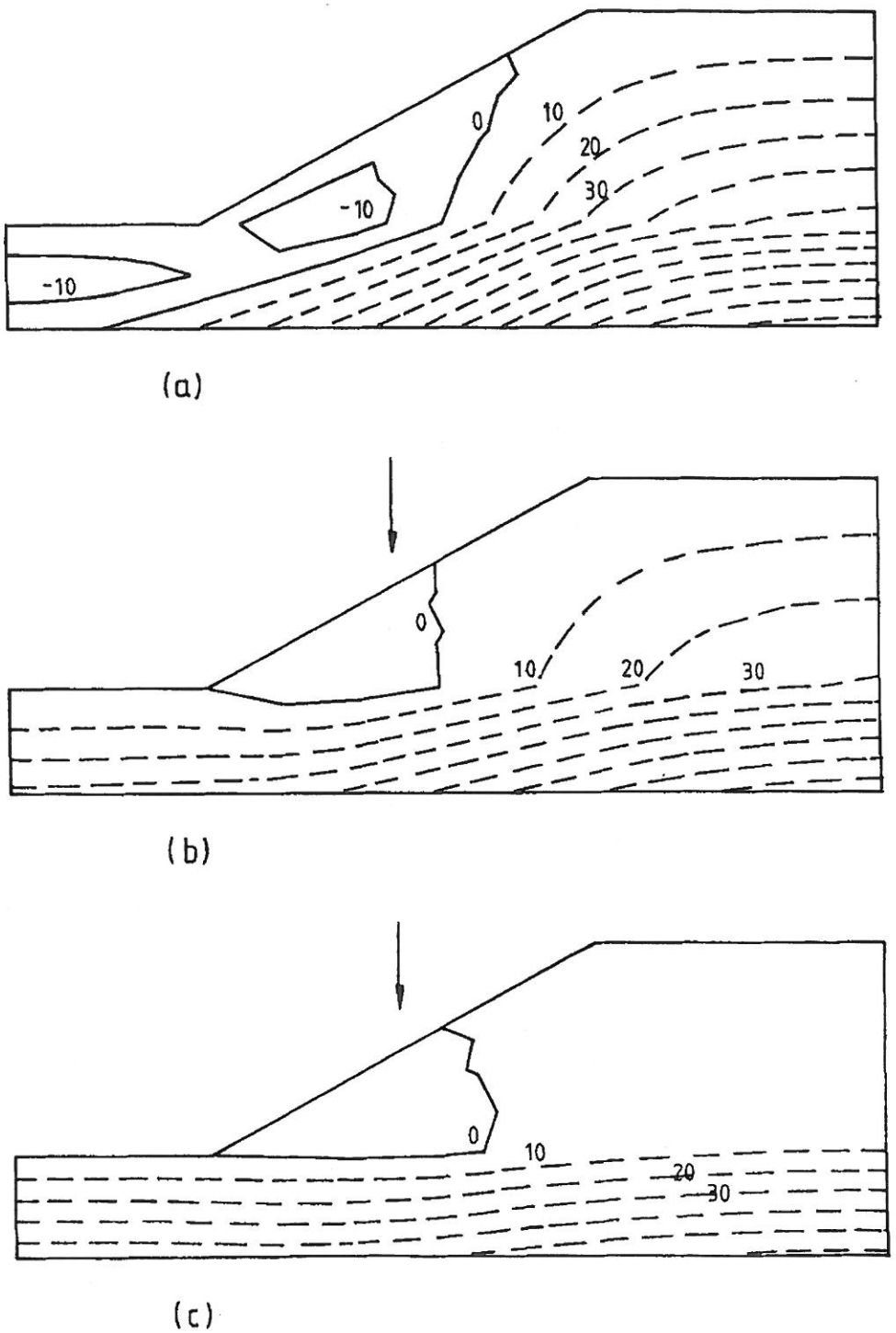


**FIG. 15. Contours of Absolute Pore Pressure (kPa), Following Excavation and Dewatering: (*a*) Immediately after Excavation; (*b*) Two Days after Excavation; and (*c*) Six Days after Excavation**

difference is explained by the fact that considerably less excess tensile pore pressure is generated when both excavation and dewatering occur simultaneously. This is due to the compensating effects of tensile pore pressures generated by the excavation, and compressive excess pore pressures generated in the fluid after the sudden lowering of the ground-water level.

Contours of absolute pore pressure at different times throughout the slope

are given in Fig. 15. It is seen that immediately after excavation and lowering of the ground water table, tensile pore pressures are generated in the region around the toe. With time, the pore pressures in this region rise as equilibrium is reached and the contours of pore pressure become increasingly horizontal as hydrostatic conditions return.

## CONCLUDING REMARKS

An elastoplastic Biot algorithm has been formulated and applied to problems of transient stability in geotechnical engineering. The algorithm was first applied to a passive earth pressure problem with a variable wall speed. It was shown to correctly model the extreme cases corresponding to fully drained and undrained behavior.

The algorithm was then applied to problems of underwater excavation. It was shown that the higher the value of $K_0$, the greater the initial stability of the excavation due to higher tensile pore pressures generated on excavation. The long-term factor of safety was found to be insensitive to the value of $K_0$, but the higher values of $K_0$ tended to delay failure of the embankment as the pore pressures took longer to dissipate. The initial stress conditions had a significant influence on the development of yielding zones and the eventual failure mechanism.

The effect of permanent drawdown on an excavation was also considered. As before, it was shown that the worst conditions occurred in the long term. The tensile pore pressure generated in the region around the toe were less than in the previous case, however, due to the compensating effect of compressive pore pressures generated in the embankment following drawdown. The smaller magnitude of the tensile pore pressure generated following excavation and drawdown, meant that failure of the embankment took less time to occur than in the case where the ground-water level remained at the crest level.

## APPENDIX I. REFERENCES


Biot, M. A. (1941). "General theory of three-dimensional consolidation." *J. Appl. Physics*, 12, 155–164.

Bishop, A. W., and Bjerrum, L. (1960). "The relevence of the triaxial test to the solution of stability problems." *Proc. ASCE Conf. on Shear Strength of Cohesive Soils*, ASCE, 437.

Bishop, A. W., and Morgenstern, N. R. (1960). "Stability coefficients for earth slopes." *Géotechnique*, 10(4), 129–150.

Bjerrum, L. (1967). "Progressive failure in slopes of consolidated plastic clay and clay shales." *J. Soil Mech. and Found. Engrg. Div.*, ASCE, 93(5), 1–49.

Griffiths, D. V. (1981). "Computation of strain softening behaviour." *Proc. Symp. on Implementation of Computer Procedures and Stress Strain Laws in Geotech. Engrg.*, C. S. Desai, and S. K. Saxena, eds., Acorn Press, Durham, N.C., 591–604.

Griffiths, D. V. (1985). The effect of pore fluid compressibility on failure loads in elastoplastic soils. *Int. J. Numer. Anal. Methods Geomech.*, 9(3), 253–259.

Griffiths, D. V., Hicks, M. A., and Li, C. O. (1991). Transient passive earth pressure analyses." *Géotechnique*, 41(4), 615–620.

Griffiths, D. V., and Li, C. O. (1989). "Accurate pore pressure calculation in undrained analysis." *Engrg. Comput. (Swansea, Wales)*, 6(4), 339–342.

Henkel, D. J. (1957). "Investigation of two long-term failures in London clay slopes at wood green and northolt." *Proc., 4th Int. Conf. Soil Mech. Foundation Engrg.*, ICSMFE, 315–320.

Hicks, M. A. (1990). "Numerically modelling the stress-strain behaviour of soils," PhD thesis, Univ. of Manchester, Manchester, United Kingdom.
Hicks, M. A., and Smith, I. M. (1986). "Influence of rate of porepressure generation on the stress-strain behaviour of soils." *Int. J. Numer. Methods Engrg.*, 22(3), 597–621.
Hwang, C. T., Morgenstern, N. R., and Murray, D. W. (1971). "On solutions of plane strain consolidation problems by finite element methods." *Can. Geotech. J.*, 8(1), 109–118.
Li, C. O. (1988). "Finite element analyses of seepage and stability problems in geomechanics," PhD thesis, University of Manchester, Manchester, United Kingdom.
Li, C. O., and Griffiths, D. V. (1988). "Finite element modelling of rapid drawdown." *Proc., 6th Int. Conf. Numerical Methods Geomech.*, G. Swoboda, ed., A. A. Balkema, Rotterdam, Netherlands, 1291–1296.
Naylor, D. J. (1974). "Stresses in nearly incompressible materials by finite elements with application to the calculation of excess pore pressure." *Int. J. Numer. Methods Engrg.*, 8(3), 443–460.
Potts, D. M., and Fourie, A. B. (1984). "The behaviour of retaining walls: results of a numerical experiment." *Géotechnique*, 34(3), 383–404.
Sandhu, R. S. (1981). "Finite element analysis of coupled deformation and fluid flow in porous media." *Numerical methods in geomechanics*, J. B. Martins, ed., D. Reidel Publishing Company, Dordrecht, Holland, 203–228.
Skempton, A. W. (1977). "Slope stability of cuttings in brown London clay." *Proc., 9th Int. Conf. Soil Mech. Foundation Engrg.*, ICSMFE, 261–270.
Small, J. C., Booker, J. R., and Davis, E. H. (1976). "Elasto-plastic consolidation of soil." *Int. J. Solids. Struct.*, 12, 431–448.
Smith, I. M., and Griffiths, D. V. (1988). *Programming finite element method.* John Wiley and Sons, 2nd Ed., New York, N.Y.
Smith, I. M., and Hobbs, R. (1976). "Biot analysis of consolidation beneath embankments." *Géotechnique*, 26(1), 149–171.
Terzaghi, K. (1936). "Stability of slopes in natural clay." *Proc., 1st Int. Conf. Soil Mech. Foundation Engrg.*, ICSMFE, 161–165.
van Leussen, W., and Nieuwenhuis, I. D. (1984). "Soil mechanics aspects of dredging." *Géotechnique*, 34(3), 359–381.
Vaughan, P. R., and Walbancke, H. J. (1973). "Pore pressure changes and delayed failure of cutting slopes in overconsolidated clay." *Géotechnique*, 23(4), 531–539.
Zienkiewicz, O. C. (1977). *The finite element method.* 3rd Ed., McGraw-Hill, New York, N.Y.
Zienkiewicz, O. C., Humpheson, C., and Lewis, R. W. (1975). "Associated and nonassociated viscoplasticity and plasticity in soil mechanics." *Géotechnique*, 25(4), 671–689.

## APPENDIX II. NOTATION

*The following symbols are used in this paper:*

$\mathbf{c}$ = element coupling matrix;
$c'$ = effective cohesion;
$c'_f$ = factored effective cohesion;
$c_v$ = coefficient of consolidation;
$E'$ = Young's modulus;
$\Delta\mathbf{f}$ = change in nodal forces;
$H$ = wall height;
$h$ = depth of Gauss point;
$K_0$ = "at-rest" earth pressure coefficient;
$k$, $k_x$, $k_y$ = coefficients of permeability;
$\mathbf{k}_m$ = element solid stiffness matrix;

$\mathbf{k}_p$ = element fluid "stiffness" matrix;
$L_R$ = wall speed parameter;
$P'_p$ = effective passive force;
$T_d$ = time factor;
$t$ = time;
$U_p$ = water force;
$u, v$ = displacements in the $x$- and $y$-directions;
$u_w$ = excess pore pressure;
$\mathbf{u}_{w_0}$ = "old" excess pore pressures;
$x, y$ = Cartesian coordinates;
$\gamma'$ = effective unit weight;
$\gamma_w$ = unit weight of water;
$\Delta\mathbf{r}$ = change in nodal displacements;
$\Delta t$ = calculation time step;
$\Delta\mathbf{u}_w$ = change in nodal excess pore pressures;
$\delta$ = horizontal wall movement;
$\theta$ = time stepping parameter;
$\nu'$ = Poisson's ratio;
$\sigma'_x$ = horizontal effective stress;
$\sigma'_y$ = vertical effective stress;
$\tau_{xy}$ = shear stress;
$\phi'$ = effective friction angle;
$\phi'_f$ = factored effective friction angle; and
$\psi'$ = dilation angle.